Bull. Chem. Soc. Jpn., 71, 2873—2884 (1998)

Steric Control of Polynuclear Manganese Complexes by the Use of Tripodal Tetradentate Ligands

Masakazu Hirotsu,* Masaaki Kojima, Wasuke Mori,† and Yuzo Yoshikawa

Department of Chemistry, Faculty of Science, Okayama University, Tsushima, Okayama 700-8530

†Department of Chemistry, Faculty of Science, Kanagawa University, 2946 Tsuchiya, Hiratsuka, Kanagawa 259-1293

(Received July 22, 1998)

Tripodal tetradentate ligands (H_2L^1: *N*,*N*-bis(2-hydroxybenzyl)-*N*′,*N*′-dimethylethylenediamine, H_2L^2: *N*-(3,5-di-*t*-butyl-2-hydroxybenzyl)-*N*-(2-hydroxybenzyl)-*N*′,*N*′-dimethylethylenediamine, H_2L^3: *N*,*N*-bis(3,5-di-*t*-butyl-2-hydroxybenzyl)-*N*′,*N*′-dimethylethylenediamine, H_2L^4: *N*,*N*-bis(2-hydroxy-3-methoxybenzyl)-*N*′,*N*′-dimethylethylenediamine, H_2L^5: *N*-(3,5-di-*t*-butyl-2-hydroxybenzyl)-*N*-(2-hydroxy-3-methoxybenzyl)-*N*′,*N*′-dimethylethylenediamine) made it possible to prepare sterically controlled polynuclear manganese complexes. In the presence of carboxylate ligands, in contrast to the L^3 ligand which gave mononuclear Mn^{III} complexes, the other ligands afforded mixed-valence trinuclear complexes with an Mn^{III}–Mn^{II}–Mn^{III} arrangement. In methanol, the general formula of the products is $[Mn_3(L)_2(carboxylato)_2(OCH_3)_2]$. While preparations in acetonitrile generated $[Mn_3(L^1)_2(ba)_4]$ (ba = benzoate(1−)) and $[Mn_3(L^2)_2(ba)_2(OH)_2]$. The structure of $[Mn_3(L^1)_2(ba)_4]$ was determined by X-ray analysis. The three manganese cores are arranged linearly, and the central and terminal ions are bridged by a phenolate and two carboxylate groups. In the case of the L^5 ligand, dinuclear and tetranuclear complexes were also obtained and structurally characterized. In the dinuclear complex, $[Mn(L^5)(CH_3OH)(OCH_3)MnCl_2]$, a distorted octahedral Mn^{III} and a five-coordinated Mn^{II} site are bridged by a phenolate and an alkoxo oxygen donor. The tetranuclear complex, $[Mn_4(L^5)_2(ba)_6]$, including an Mn^{III}–Mn^{II}–Mn^{II}–Mn^{III} arrangement, is regarded as a carboxylato bridged dimer of a dinuclear unit, $[Mn(L^5)(ba)_2Mn]^+$. Because the bulkiness of the L^5 ligand lies between the L^2 and L^3 ligands, the dinuclear unit is favorable. Variable-temperature magnetic susceptibility measurements showed the ferromagnetic spin-exchange coupling for $[Mn(L^5)(CH_3OH)(OCH_3)MnCl_2]$ and the antiferromagnetic one for $[Mn_3(L^1)_2(ba)_4]$. The phenolato and alkoxo bridges give rise to the ferromagnetic exchange interactions between Mn^{III} and Mn^{II} ions. On the other hand, the antiferromagnetic interactions stem from carboxylato bridges.

Polynuclear manganese complexes have been prepared as model compounds of redox-active enzymes.[1,2] A dinuclear manganese site has been shown for a variety of enzymes such as manganese catalases,[3] and tetranuclear manganese complexes are important for the water oxidation center of photosystem II.[4] Kessissoglou et al. prepared several mixed-valence trinuclear complexes.[5—7] The complexes are generated as a result of spontaneous self-assembly, and mostly contain a linear Mn^{III}–Mn^{II}–Mn^{III} arrangement. Recently, we reported on trinuclear complexes with the same arrangement using tetradentate ligands, L^1 and L^2, which are depicted in Chart 1.[8] The compounds consist of the terminal Mn^{III}(L) units and the central manganese(II) core and they are supported by additional bridging ligands. On the other hand, the L^3 ligand gave only mononuclear manganese complexes. The bulkiness of the 3-positioned *t*-butyl groups on the aromatic rings prevent the formation of polynuclear manganese complexes. In self-assembly, the structure of a product strongly reflects the steric factors of each fragment. If we can control the steric factors, we may expect the formation of the di- and tetranuclear manganese complexes. Therefore, we thought about adjusting the tripodal tetradentate ligand and the reaction conditions.

In this work, we reveal the sterically controlled formation of the polynuclear manganese complexes with the tripodal tetradentate ligands. In order to control the steric effect of the coordination environment, several kinds of functional groups were introduced to the aromatic rings of the ligand, as shown in Chart 1. The mixed-valence polynuclear complexes were obtained with Mn^{III}–Mn^{II}, Mn^{III}–Mn^{II}–Mn^{III}, and Mn^{III}–Mn^{II}–Mn^{II}–Mn^{III} arrangements. The structures of the di-, tri-, and tetranuclear complexes were determined by X-ray analysis. For the mixed-valence polynuclear complexes, the temperature-dependent magnetic behavior was examined.

Experimental

Abbreviations. Abbreviations of the tripodal ligands are represented in Chart 1: H_2L^6 = *N*,*N*-bis(2-hydroxybenzyl)-(2-pyridyl)-methylamine. The following abbreviations are used in this paper: Hsal = salicylaldehyde, Hacac = acetylacetone, Hba = benzoic acid, Hmcba = *m*-chlorobenzoic acid, and Hbf = benzoylformic acid.

Ligands. Tripodal ligands were prepared by a modification of the method reported by Hinshaw et al.[9] A representative procedure for H_2L^2 is available in the literature.[8] The ligand H_2L^5 was prepared by the same method as that for H_2L^2 except that 3-methoxysalicylaldehyde was used instead of salicylaldehyde. The

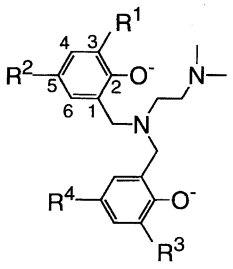

	R^1	R^2	R^3	R^4
L^1	H	H	H	H
L^2	*t*-Bu	*t*-Bu	H	H
L^3	*t*-Bu	*t*-Bu	*t*-Bu	*t*-Bu
L^4	OCH_3	H	OCH_3	H
L^5	*t*-Bu	*t*-Bu	OCH_3	H

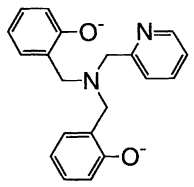

L^6

Chart 1.

yield was 46%. ^{1}H NMR (500 MHz, $CDCl_3$) δ = 1.26 (s, 9H), 1.34 (s, 9H), 2.33 (s, 6H), 2.59 (m, 4H), 3.59 (s, 2H), 3.70 (s, 2H), 3.89 (s, 3H), 6.71—6.85 (m, 4H), 7.16 (d, 1H).

[Mn(L^1)(sal)] (1a), [Mn(L^2)(sal)]·H_2O (1b), [Mn(L^3)(sal)] (1c), and [Mn(L^3)(acac)] (1d). Complex **1d** was as reported in a preceding paper.[8] The other complexes were prepared by a similar method, and a representative procedure is given for **1a**. The H_2L^1 ligand (0.150 g, 0.5 mmol) was added to a solution of $MnCl_2·4H_2O$ (0.099 g, 0.5 mmol) in methanol (10 cm^3), and the reaction mixture was stirred. To the resulting brown solution was added a methanol solution (5 cm^3) of salicylaldehyde (0.122 g, 1 mmol). A 0.5 M (1 M = 1 mol dm^{-3}) solution (2 cm^3) of NaOH in methanol was then added dropwise to the stirred solution. The resulting dark brown solution was stirred for 1 h, and allowed to stand. A dark brown precipitate was deposited, collected by filtration, and washed with methanol. The crude product was recrystallized from dichloromethane–methanol, and dried over P_4O_{10} under vacuum. The yield was 0.130 g (55%) of **1a**. μ_{eff} (294 K) 4.94 μ_B. Anal. Found: C, 63.23; H, 5.82; N, 5.97%. Calcd for $C_{25}H_{27}MnN_2O_4$: C, 63.29; H, 5.74; N, 5.90%.

[Mn(L^2)(sal)]·H_2O (**1b**). Yield: 67%. μ_{eff} (294 K) 4.89 μ_B. Anal. Found: C, 65.97; H, 7.44; N, 4.65%. Calcd for $C_{33}H_{45}MnN_2O_5$: C, 65.55; H, 7.50; N, 4.63%. A piece of the crystal was used for the X-ray crystal structure determination.

[Mn(L^3)(sal)] (**1c**). Yield: 70%. μ_{eff} (294 K) 4.87 μ_B. Anal. Found: C, 70.30; H, 8.49; N, 3.98%. Calcd for $C_{41}H_{59}MnN_2O_4$: C, 70.46; H, 8.51; N, 4.01%.

[Mn_3(L^4)$_2$(mcba)$_2$(OCH_3)$_2$] (2). The H_2L^4 ligand (0.180 g, 0.5 mmol) and *m*-chlorobenzoic acid (0.078 g, 0.5 mmol) was added to a solution of $MnCl_2·4H_2O$ (0.148 g, 0.75 mmol) in methanol (10 cm^3), and the reaction mixture was stirred. *N*,*N*-Diisopropylethylamine (0.340 cm^3, 2.0 mmol) was added, and the resulting dark green solution was stirred for 3 h. A dark green solid was precipitated, collected by filtration, and washed with methanol. The product was recrystallized from dichloromethane–methanol and dried over P_4O_{10} under vacuum to yield 0.209 g (67%) of **2**. μ_{eff} (294 K) 9.4 μ_B. IR (KBr pellet) ν_{as}(COO) 1604, ν_s(COO) 1384 cm^{-1}. UV-vis (CH_2Cl_2) 23100 cm^{-1} (ε 2160 M^{-1} cm^{-1}). Anal. Found: C, 53.01; H, 5.32; N, 4.53%. Calcd for $C_{56}H_{66}Cl_2Mn_3N_4O_{14}$: C, 53.60; H, 5.30; N, 4.46%.

[Mn_3(L^5)$_2$(mcba)$_2$(OCH_3)$_2$]·$2H_2O$ (3). The H_2L^5 ligand (0.133 g, 0.3 mmol) and *m*-chlorobenzoic acid (0.047 g, 0.3 mmol) were added to a solution of $Mn(ClO_4)_2·6H_2O$ (0.163 g, 0.45 mmol) in methanol (10 cm^3), and the reaction mixture was stirred. *N*,*N*-Diisopropylethylamine (0.204 cm^3, 1.2 mmol) was added, and the resulting dark brown solution was stirred for 3 h. A dark brown solid was precipitated, collected by filtration, and washed with methanol. The product was recrystallized from dichloromethane–methanol and dried over P_4O_{10} under vacuum to yield 0.133 g (61%) of **3**. μ_{eff} (299 K) 9.26 μ_B. IR (KBr pellet) ν_{as}(COO) 1602, ν_s(COO) 1386 cm^{-1}. Anal. Found: C, 57.33; H, 6.62; N, 3.90%. Calcd for $C_{70}H_{98}Cl_2Mn_3N_4O_{14}$: C, 57.77; H, 6.79; N, 3.85%.

[Mn(L^5)(CH_3OH)(OCH_3)$MnCl_2$]·CH_3OH (4). The H_2L^5 ligand (0.221 g, 0.5 mmol) was added to a solution of $MnCl_2·4H_2O$ (0.198 g, 1.0 mmol) in methanol (15 cm^3), and the reaction mixture was stirred. To the resulting reddish brown solution, a 0.5 M solution (2.0 cm^3) of NaOH in methanol was added dropwise with stirring. The solution turned dark brown. After stirring for 1 h, a dark brown solid was precipitated, collected by filtration, and washed with methanol. The crude product was recrystallized from dichloromethane-methanol to yield 0.167 g (47%) of **4**. μ_{eff} (295 K) 8.06 μ_B. Anal. Found: C, 50.35; H, 6.80; N, 4.33%. Calcd for $C_{30}H_{51}Cl_2Mn_2N_2O_6$: C, 50.29; H, 7.17; N, 3.91%. Crystals suitable for the X-ray structure determination were obtained by the following procedure. To a filtrated solution of H_2L^5 (0.221 g, 0.5 mmol) and $MnCl_2·4H_2O$ (0.198 g, 1.0 mmol) in methanol (20 cm^3) was added *N*,*N*-diisopropylethylamine (0.170 cm^3, 1.0 mmol). The solution was allowed to stand. Brown plates were deposited as X-ray quality crystals.

[Mn_3(L^1)$_2$(ba)$_4$] (5). The H_2L^1 ligand (0.150 g, 0.5 mmol), benzoic acid (0.122 g, 1.0 mmol), and $Mn(ClO_4)_2·6H_2O$ (0.271 g, 0.75 mmol) were dissolved in acetonitrile (10 cm^3), and the reaction mixture was stirred. To the solution, *N*,*N*-diisopropylethylamine (0.340 cm^3, 2.0 mmol) was added with stirring. The solution turned dark brown. After stirring for 3 h, a dark brown solid was precipitated, collected by filtration, and washed with acetonitrile. The crude product was recrystallized from dichloromethane-acetonitrile to yield 0.171 g (55%) of **5**. μ_{eff} (295 K) 8.60 μ_B. IR (KBr pellet) ν_{as}(COO) 1606, ν_s(COO) 1396 cm^{-1}. Anal. Found: C, 61.36; H, 5.30; N, 4.84%. Calcd for $C_{64}H_{64}Mn_3N_4O_{12}$: C, 61.69; H, 5.18; N, 4.50%. A piece of the crystal was used for the X-ray crystal structure determination.

[Mn_3(L^2)$_2$(ba)$_2$($OH)_2$]·H_2O (6). The H_2L^2 ligand (0.206 g, 0.5 mmol), benzoic acid (0.122 g, 1.0 mmol), and $Mn(ClO_4)_2·6H_2O$ (0.271 g, 0.75 mmol) were dissolved in acetonitrile (10 cm^3), and the reaction mixture was stirred. To the solution, *N*,*N*-diisopropylethylamine (0.340 cm^3, 2.0 mmol) was added with stirring. The solution turned dark brown. After stirring for 3 h, a dark brown solid was precipitated, collected by filtration, and washed with acetonitrile. The crude product was recrystallized from dichloromethane–acetonitrile to yield 0.280 g (87%) of **6**. μ_{eff} (294 K) 8.7 μ_B. IR (KBr pellet) ν(OH) 3662, ν_{as}(COO) 1601, ν_s(COO) 1393 cm^{-1}. Anal. Found: C, 61.98; H, 7.10; N, 4.62%. Calcd for $C_{66}H_{90}Mn_3N_4O_{11}$:

C, 61.92; H, 7.09; N, 4.38%. Deuteration of OH groups was carried out. The complex **6** (62 mg) was added in dichloromethane–acetonitrile (30 cm^3/10 cm^3) with D_2O (0.100 cm^3). The suspension was stirred for 3 h, and concentrated by rotary evaporation. The resulting dark brown precipitate was collected by filtration and washed with acetonitrile to obtain 43 mg of the partially deuterated compound. IR (KBr pellet) ν(OH) 3662, ν(OD) 2702 cm^{-1}.

[Mn(L^3)(mcba)(H_2O)]·H_2O (7). The H_2L^3 ligand (0.157 g, 0.3 mmol), *m*-chlorobenzoic acid (0.094 g, 0.6 mmol), and Mn(ClO_4)$_2$·$6H_2O$ (0.163 g, 0.45 mmol) were dissolved in acetonitrile (10 cm^3), and the reaction mixture was stirred. To the solution, *N,N*-diisopropylethylamine (0.204 cm^3, 1.2 mmol) was added with stirring. The resulting deep purple mixture was stirred for 3 h. A purple solid was precipitated, collected by filtration, and washed with acetonitrile. The crude product was recrystallized from dichloromethane–acetonitrile to yield 0.145 g (63%) of **7**. IR (KBr pellet) ν_{as}(COO) 1602, ν_s(COO) 1366 cm^{-1}. Anal. Found: C, 64.18; H, 8.41; N, 4.09%. Calcd for $C_{41}H_{62}ClMnN_2O_6$: C, 64.01; H, 8.12; N, 3.64%.

[Mn_4(L^5)$_2$(ba)$_6$] (8). The H_2L^5 ligand (0.133 g, 0.3 mmol), benzoic acid (0.073 g, 0.6 mmol), and Mn(ClO_4)$_2$·$6H_2O$ (0.163 g, 0.45 mmol) were dissolved in acetonitrile (10 cm^3), and the reaction mixture was stirred. To the solution, *N,N*-diisopropylethylamine (0.204 cm^3, 1.2 mmol) was added with stirring. The solution turned dark brown. After stirring for 3 h, a purple solid was precipitated, collected by filtration, and washed with acetonitrile. The crude product was recrystallized from dichloromethane-acetonitrile to yield 0.117 g (64%) of **8**. IR (KBr pellet) ν_{as}(COO) 1603, ν_s(COO) 1399 cm^{-1}. Anal. Found: C, 62.53; H, 6.18; N, 2.77%. Calcd for $C_{96}H_{110}Mn_4N_4O_{18}$: C, 63.09; H, 6.07; N, 3.07%.

[Mn_3(L^1)$_2$(mcba)$_2$(OC_2H_5)$_2$]·H_2O (9). The H_2L^1 ligand (0.150 g, 0.5 mmol) was added to a solution of Mn(ClO_4)$_2$·$6H_2O$ (0.362 g, 1.0 mmol) in ethanol (10 cm^3). To this solution was added *m*-chlorobenzoic acid (0.157 g, 1.0 mmol), and the reaction mixture was stirred. An ethanol solution (5 cm^3) of *N,N*-diisopropylethylamine (0.388 g, 3.0 mmol) was added dropwise with stirring, and the solution turned dark green. After stirring for 5 h, a dark brown solid was precipitated, collected by filtration, and washed with ethanol. The crude product was recrystallized from dichloromethane–ethanol to give dark brown crystals of **9**. The yield was 0.184 g (62%). IR (KBr pellet) ν_{as}(COO) 1596, ν_s(COO) 1387 cm^{-1}. μ_{eff} (295 K) 9.19 μ_B. Anal. Found: C, 54.87; H, 5.48; N, 4.78%. Calcd for $C_{54}H_{64}Cl_2Mn_3N_4O_{11}$: C, 54.93; H, 5.46; N, 4.74%.

[Mn_3(L^6)$_2$(mcba)$_2$(OC_2H_5)$_2$] (10). The H_2L^6 ligand (0.160 g, 0.5 mmol) was added to a solution of Mn(ClO_4)$_2$·$6H_2O$ (0.362 g, 1.0 mmol) in ethanol (10 cm^3). To this solution was added *m*-chlorobenzoic acid (0.157 g, 1.0 mmol), and the reaction mixture was stirred. An ethanol solution (5 cm^3) of *N,N*-diisopropylethylamine (0.323 g, 2.5 mmol) was added dropwise with stirring, and the solution turned dark green. After stirring for 5 h, a dark brown solid was precipitated, collected by filtration, and washed with ethanol. The crude product was recrystallized from dichloromethane–ethanol to yield 0.238 g (79%) of **10**. IR (KBr pellet) ν_{as}(COO) 1596, ν_s(COO) 1386 cm^{-1}. μ_{eff} (298 K) 9.14 μ_B. Anal. Found: C, 57.62; H, 4.65; N, 4.70%. Calcd for $C_{58}H_{54}Cl_2Mn_3N_4O_{10}$: C, 57.92; H, 4.53; N, 4.66%.

Physical Measurements. Visible-UV absorption spectra were recorded with a JASCO Ubest-550 spectrophotometer. Infrared spectra were recorded with a JASCO IR-810 spectrophotometer. Magnetic susceptibility data in the 2—300 K temperature range were collected using a SQUID magnetometer (Quantum Design, MPMS-5S). The values of the applied magnetic field strength were 0.2 T for **4**, **9**, and **10**; 0.1 T for **5**. Room-temperature magnetic susceptibilities were measured with a Sherwood Scientific Ltd., Model MK1 magnetic susceptibility balance. The susceptibilities were corrected for diamagnetism estimated from Pascal's constants. ^{1}H NMR spectra were measured on a Varian VXR-200 or a Varian VXR-500 spectrometer. Elemental analyses were carried out on a Parkin–Elmer 2400 II elemental analyzer.

Collection and Reduction of X-Ray Data. Diffraction measurements were made on a Rigaku AFC-5S diffractometer at Institute for Molecular Science for **1b** and a Rigaku AFC-5R diffractometer at the X-ray Laboratory of Okayama University for **4**, **5**, and **8** using graphite-monochromated Mo $K\alpha$ radiation. A brown prismatic crystal of **1b**, a brown plate of **4**, a brown prismatic crystal of **5**, and a brown plate of **8** were mounted. Crystallographic data are given in Table 1. The cell parameters were obtained by a least-squares refinement of the angular settings of 25 reflections in the range of $18° < 2\theta < 23°$. Data collections were carried out using the ω scan technique ($2\theta < 55°$ for **1b**, $2\theta < 52°$ for **4**, $2\theta < 48°$ for **5**, and $2\theta < 47°$ for **8**). During the data collection, the intensities of three standard reflections were measured after every 97 reflections and showed no significant reduction. An empirical absorption correction based on ψ scans of three reflections was applied for **1b**, **4**, and **8**. All calculations were carried out using the TEXSAN[10] crystallographic software package on a VAX workstation. The structure was solved by direct methods for **1b** and a heavy-atom Patterson method for **4**, **5**, and **8**, and expanded using Fourier techniques. All non-hydrogen atoms were refined anisotropically by a full-matrix least-squares procedure. In **4**, hydrogen atoms were refined isotropically, except for those of the *t*-butyl and methoxy groups on the L^5 ligand and the uncoordinated methanol molecule. The hydrogen atoms of the solvent of crystallization were not included (**1b** and **4**). The other hydrogen atoms were included, but not refined, and were placed at fixed distances of 0.95 Å from bonded carbon atoms. The maximum and minimum peaks on the final difference Fourier map corresponded to 0.30 and −0.27 e Å^{-3} for **1b**, 0.51 and −0.40 e Å^{-3} for **4**, 0.64 and −0.62 e Å^{-3} for **5**, and 0.49 and −0.51 e Å^{-3} for **8**.

For **1b**, **4**, **5**, and **8**, full crystallographic data, experimental details, atomic coordinates and equivalent isotropic temperature factors for all atoms, anisotropic temperature factors for non-hydrogen atoms, complete bond distances and angles, tables of observed and calculated structure factors, and fully labeled ORTEP diagrams are deposited as Document No. 71069 at the Office of the Editor of Bull. Chem. Soc. Jpn.

Results and Discussion

Mononuclear Unit, [Mn(L)(solvent)$_2$]$^+$. In a methanol solution, the ligation of the tripodal tetradentate ligand (L) to manganese(II) species ([Mn(solvent)$_6$]$^{2+}$) facilitates the oxidation to manganese(III) species by air. Furthermore, the addition of didentate ligands, such as salicylaldehyde and acetylacetone, gave mononuclear manganese(III) complexes, [Mn(L^1)(sal)] (**1a**), [Mn(L^2)(sal)] (**1b**), [Mn(L^3)(sal)] (**1c**), and [Mn(L^3)(acac)] (**1d**). Because the manganese(III) mononuclear unit with the L ligand is the key component in this work, the structure and spectroscopic properties were examined.

Figure 1 shows a perspective view of the structure of [Mn(L^2)(sal)] (**1b**). The selected bond distances and angles are

Table 1. Crystallographic Data for $[Mn(L^1)(sal)]\cdot H_2O$ (**1b**), $[Mn(L^5)(CH_3OH)(OCH_3)MnCl_2]\cdot CH_3OH$ (**4**), $[Mn_3(L^1)_2(ba)_4]$ (**5**), and $[Mn_4(L^5)_2(ba)_6]$ (**8**)

	1b	**4**	**5**	**8**
Formula	$C_{33}H_{45}MnN_2O_5$	$C_{31}H_{51}Cl_2Mn_2N_2O_6$	$C_{64}H_{64}Mn_3N_4O_{12}$	$C_{96}H_{110}Mn_4N_4O_{18}$
Fw	604.67	716.52	1246.04	1827.70
Crystal system	Orthorhombic	Monoclinic	Monoclinic	Monoclinic
Space group	$P2_12_12_1$ (No. 19)	$P2_1/c$ (No. 14)	$P2_1/n$ (No. 14)	$P2_1/n$ (No. 14)
a/Å	11.663(2)	10.039(2)	14.163(3)	20.371(8)
b/Å	31.775(8)	15.369(2)	17.347(7)	9.424(4)
c/Å	8.831(3)	23.398(3)	24.593(5)	25.755(8)
β/deg		94.95(1)	105.72(2)	111.22(3)
V/Å^3	3273(2)	3597(2)	5816(5)	4609(6)
Z	4	4	4	2
D_{calcd}/g cm^{-3}	1.227	1.323	1.423	1.317
λ/Å	0.7107 (Mo $K\alpha$)	0.7107 (Mo $K\alpha$)	0.7107 (Mo $K\alpha$)	0.7107 (Mo $K\alpha$)
μ/mm^{-1}	0.425	0.862	0.680	0.579
Crystal size/mm	$0.32\times0.28\times0.60$	$0.60\times0.05\times0.61$	$0.15\times0.10\times0.45$	$0.26\times0.07\times0.40$
T/°C	23	26	25	25
No. of unique data	4279	7353	9479	7306
No. of observations	2308 ($I>2.0\sigma(I)$)	4172 ($I>2.0\sigma(I)$)	3568 ($I>2.0\sigma(I)$)	2827 ($I>2.0\sigma(I)$)
No. of variables	370	483	748	550
R[a)]	0.051	0.057	0.082	0.073
R_w[b)]	0.047	0.050	0.060	0.070

a) $R = \sum||F_o| - |F_c||/\sum|F_o|$. b) $R_w = [\sum w(|F_o| - |F_c|)^2/\sum wF_o^2]^{1/2}$, $w = 1/\sigma^2(F_o)$.

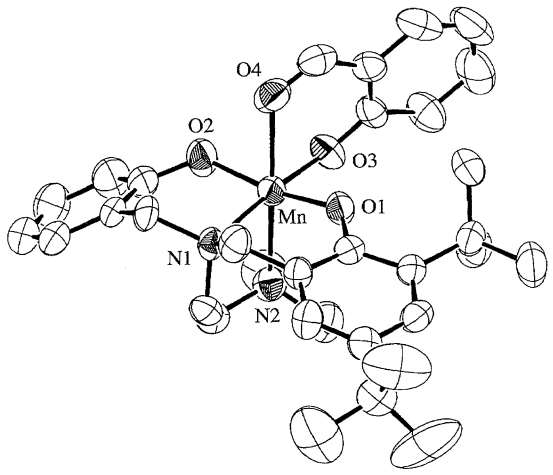

Fig. 1. ORTEP view of $[Mn(L^2)(sal)]$ (**1b**) with thermal ellipsoids of 50% probability.

Table 2. Selected Bond Distances (Å) and Angles (deg) for $[Mn(L^1)(sal)]\cdot H_2O$ (**1b**)

Mn–O(1)	1.873(4)	Mn–O(4)	2.275(5)
Mn–O(2)	1.906(4)	Mn–N(1)	2.088(4)
Mn–O(3)	1.915(4)	Mn–N(2)	2.350(6)
O(1)–Mn–O(2)	169.2(2)	O(2)–Mn–N(2)	91.1(2)
O(1)–Mn–O(3)	89.5(2)	O(3)–Mn–O(4)	85.0(2)
O(1)–Mn–O(4)	84.2(2)	O(3)–Mn–N(1)	172.6(2)
O(1)–Mn–N(1)	91.3(2)	O(3)–Mn–N(2)	91.5(2)
O(1)–Mn–N(2)	99.6(2)	O(4)–Mn–N(1)	102.5(2)
O(2)–Mn–O(3)	88.9(2)	O(4)–Mn–N(2)	174.8(2)
O(2)–Mn–O(4)	85.0(2)	N(1)–Mn–N(2)	81.1(2)
O(2)–Mn–N(1)	91.7(2)		

given in Table 2. The manganese(III) center is in a distorted octahedral environment. The equatorial plane is composed of a tertiary amine nitrogen and three phenolate oxygen donors. The remaining terminal nitrogen and the aldehyde oxygen occupy the axial positions. The three Mn–O(phenolato) distances of 1.873(4), 1.906(4), and 1.915(4) Å are comparable; these distances are located within the range of those for Mn^{III} complexes reported.[11—13] From the effective magnetic moment (4.89 μ_B at 294 K), **1b** is the high-spin d^4 compound, and the large axial bond lengths, Mn–O(4) (2.275(5) Å) and Mn–N(2) (2.350(6) Å), are consistent with a Jahn–Teller distortion. The structure related to the coordination bonds with the tripodal tetradentate ligand, L^2, is very similar to that of $[Mn(L^3)(mcba)(CH_3OH)]$.[8] The tripodal tetradentate ligands maintain the coordination environment around an Mn^{III} ion irrespective of the substituents and the additional ligands.

Figure 2 shows electronic absorption spectral changes of a dichloromethane–methanol solution (1 : 4, v/v) of $[Mn(L^2)(sal)]$ (**1b**) on addition of $Mn(ClO_4)_2\cdot 6H_2O$ (0—12 equiv). For other compounds (**1a**, **1c**, and **1d**), similar spectral changes were observed. All spectra showed isosbestic points, and two intense bands appeared. The maxima are λ_1 = 486 nm (20.6×10^3 cm^{-1}), λ_2 = 370 nm (27.0×10^3 cm^{-1}) for **1a**; λ_1 = 499 nm (20.0×10^3 cm^{-1}), λ_2 = 376 nm (26.6×10^3 cm^{-1}) for **1b**; and λ_1 = 515 nm (19.4×10^3 cm^{-1}), λ_2 = 383 nm (26.1×10^3 cm^{-1}) for **1c** and **1d**. These results indicate that an equilibrium exists between the Mn^{III} complexes and the Mn^{II} ion (absorption of the excess Mn^{II} ion is negligible because of the small extinction coefficient). The same values of two maxima (λ_1 and λ_2) for complexes **1c** and **1d** indicate that the species responsible for the new bands are independent of the didentate ligands. Therefore,

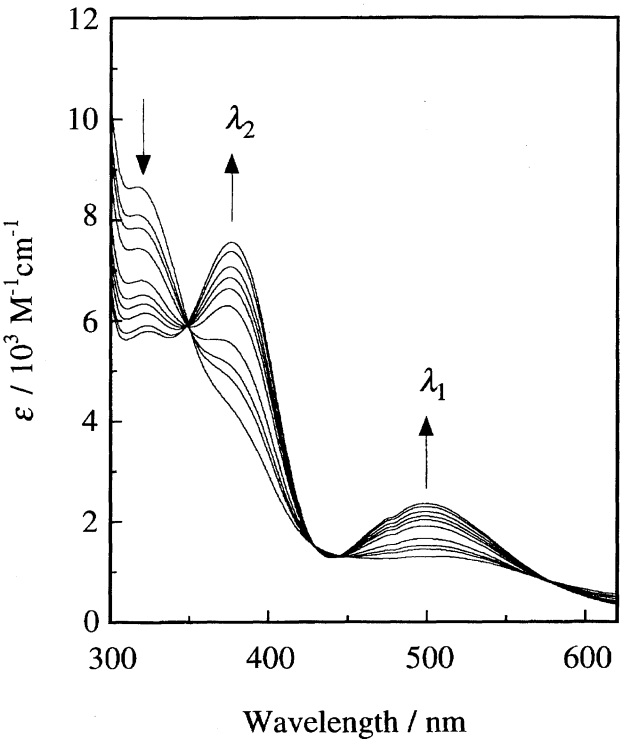

Fig. 2. Electronic absorption spectral changes for a reaction of [Mn(L^2)(sal)] (**1b**) (1.0 equiv) with $Mn(ClO_4)_2 \cdot 6H_2O$ (0, 0.2, 0.3, 0.5, 1.0, 1.5, 2.0, 3.0, 6.0, 12.0 equiv) in dichloromethane–methanol (1 : 4, v/v).

we suggest that the didentate ligands of the Mn^{III} complexes are easily dissociated and transferred to the Mn^{II} ion. The equilibrium is given by Eq. 1 in which X represents the anion of the didentate ligand, salicylaldehyde or acetylacetone.

$$[Mn^{III}(L)(X)] + [Mn^{II}(solvent)_6]^{2+} \rightleftarrows [Mn^{III}(L)(solvent)_2]^{+} + [Mn^{II}(solvent)_4(X)]^{+} \quad (1)$$

The two growing bands stem from the $[Mn^{III}(L)(solvent)_2]^+$ cation. These bands with large extinction coefficients are assigned to an LMCT transition from a pπ orbital on the phenolate oxygen to the manganese(III) dπ* orbitals as reported for other manganese(III) complexes.[11] The species with electron-donating *t*-butyl groups exhibit the bands at lower energy than does the non-substituted one (λ_1, λ_2/nm: **1a** < **1b** < **1c**, **1d**). A similar phenomenon has been reported for (thiophenolato)iron(II) complexes (a thiolate to iron charge transfer).[14] On the other hand, an opposite trend has been reported for MLCT bands of (α-ketocarboxylato)-iron(II) complexes.[15]

Trinuclear Manganese Complexes with Phenolato, Carboxylato, and Alkoxo Bridges. In the case of the L^1 and L^2 ligands, the formation of the mixed-valence trinuclear manganese complexes is observed, as previously described.[8] Generally, the reaction of a manganese(II) salt with a tripodal ligand (H_2L^1 or H_2L^2), carboxylic acid, and a base in methanol affords a trinuclear manganese complex, $[Mn_3(L)_2(carboxylato)_2(OCH_3)_2]$. On the basis of the manganese(III) species observed in Eq. 1, the formation of these trinuclear complexes ($[\{Mn^{III}(L)(carboxylato)(OCH_3)\}_2Mn^{II}]$) in a basic methanol solution is interpreted as the result of the association of the two $[Mn^{III}(L)(solvent)_2]^+$ cations with $[Mn^{II}(solvent)_6]^{2+}$. On the other hand, the L^3 ligand gave only the mononuclear manganese complex, [Mn(L^3)(carboxylato)(CH_3OH)]. In the latter case, the 3-positioned *t*-butyl groups on the aromatic rings prevent the phenolate oxygen donor from bridging two manganese cores. Figure 3 shows steric interactions in the trinuclear complex. Two repulsive interactions are important, and both are related to the 3-positioned substituents; one is between the bridging ligand and the R^1 substituent, the other is between the bridging ligand and the R^3 substituent. In the L^2 ligand, the alkoxo bridge of the trinuclear complex interacts with only one substituent, R^1. If both R^1 and R^3 are replaced by bulkier groups, more effective repulsion is expected. In order to examine the steric effect of the substituent, we prepared the L^4 ligand which contains two 3-positioned methoxy groups at R^1 and R^3. The elemental analysis and the UV-vis spectrum of the reaction product with this ligand indicate that the structure is similar to those of the previously reported mixed-valence trinuclear complexes, $[Mn_3(L^1)_2(mcba)_2(OCH_3)_2]$ and $[Mn_3(L^2)_2(mcba)_2(OCH_3)_2]$.[8] The effective magnetic moment of the complex with L^4 is 9.4 μ_B at 294 K. This value is close to the theoretical spin-only value of 9.11 μ_B for an uncoupled 2-5/2-2 spin system corresponding to the Mn^{III}–Mn^{II}–Mn^{III} arrangement. From these results, we identified this complex as the mixed-valence trinuclear complex, $[Mn_3(L^4)_2(mcba)_2(OCH_3)_2]$ (**2**). This implies that the methoxy group is too small to prevent the formation of the trinuclear complex.

Next, we prepared the L^5 ligand which contains an additional 3-positioned methoxy group to the L^2 ligand. Clearly, the steric effect of the L^5 ligand is larger than that of L^2 and L^4. As shown in Fig. 3, the substituents of L^5 provide the crowded surroundings for the bridging ligand, and may prevent the formation of the trinuclear complex. However, the preparation with this ligand also afforded the trinuclear complex, $[Mn_3(L^5)_2(mcba)_2(OCH_3)_2]$ (**3**). Consequently, all of the tripodal tetradentate ligands, except for L^3, gave the analogous trinuclear complexes. In order to control the number of manganese cores, finer tuning of the steric effect

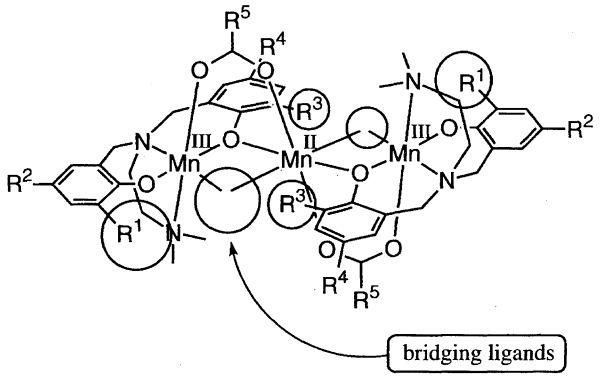

Fig. 3. Steric interactions of mixed-valence trinuclear manganese complexes.

is needed.

Dinuclear Manganese Complex with Phenolato and Alkoxo Bridges. As a second step to control the number of manganese cores, we removed a carboxylate ligand from the reaction system. The reaction of $MnCl_2 \cdot 4H_2O$ (2 equiv) with H_2L^5 (1 equiv), and a base (NaOH or *N*,*N*-diisopropylethylamine, 2 equiv) in methanol gave a brown crystalline product. We inferred a dinuclear structure from elemental analysis and the effective magnetic moment.

The structure of the dinuclear complex, $[Mn(L^5)(CH_3OH)(OCH_3)MnCl_2] \cdot CH_3OH$ (**4**), was revealed by X-ray crystal structure analysis. Figure 4 shows a view of the molecular structure, and the selected bond distances and angles are given in Table 3. Two manganese cores are bridged by a phenolate and an alkoxide group. One manganese ion is coordinated by the L^5 ligand, the alkoxide group, and a methanol molecule. The manganese ion is in the axially elongated octahedral environment, which consists of N(1), O(1), O(2), and O(4) in an equatorial plane and N(2) and O(5) in the axial positions. This is consistent with a Jahn–Teller distortion of a high-spin d^4 electron configuration, as in the case of the mononuclear complex **1b**. The other manganese ion is coordinated by a phenolate and an alkoxide group, two chloride ions, and the methoxy group on the L^5 ligand. The distances of the two bridging bonds, Mn(2)–O(2) and Mn(2)–O(4), are longer than those of Mn(1)–O(2) and Mn(1)–O(4) in the former site. Therefore, the oxidation state of Mn(1) surrounded by the L^5 ligand is assigned to Mn^{III}, and that of the five coordination site (Mn(2)) to Mn^{II}.

The comparison between the dinuclear and trinuclear complexes indicates a significant similarity about the bridging structure. In the dinuclear complex **4**, the Mn^{III}–O(phenolato)–Mn^{II} angle is 103.3(1)° and the Mn^{III}–O(alkoxo)–Mn^{II} angle is 106.2(1)° and both values are similar to those of the mixed-valence trinuclear manganese complexes, 99° and 102° (average), which are previously reported for $[Mn_3(L^1)_2(mcba)_2(OCH_3)_2]$, $[Mn_3(L^2)_2(mcba)_2(OCH_3)_2]$, and $[Mn_3(L^1)_2(bf)_2(OCH_3)_2]$.[8] The sum of the bond angles around the bridging oxygen donor is about 360° in both the phenolato and alkoxo bridges, as is the case with the trinuclear complexes. The oxygen which bridges Mn^{III} and Mn^{II} becomes sp^2-hybridization. The distance between the Mn^{III} and Mn^{II} cores in **4** is 3.210(1) Å, and the average of those in the trinuclear complexes is 3.16 Å. The similar outlines of bridging frames indicate that the structures of these complexes are based on the phenolato and alkoxo bridges. The carboxylato bridges support the formation of the polynuclear complexes in methanol. In the case of the L^5 ligand, di- and trinuclear species ($[Mn(L^5)(OCH_3)Mn]^{2+}$ and $[\{Mn(L^5)(OCH_3)\}_2Mn]^{2+}$) coexist in methanol. The carboxylate ligand serves to isolate the trinuclear complex from the mixture.

Table 3. Selected Bond Distances (Å) and Angles (deg) for $[Mn(L^5)(CH_3OH)(OCH_3)MnCl_2] \cdot CH_3OH$ (**4**)

Mn(1)–O(1)	1.872(3)	Mn(2)–Cl(1)	2.347(2)
Mn(1)–O(2)	1.935(3)	Mn(2)–Cl(2)	2.344(2)
Mn(1)–O(4)	1.905(3)	Mn(2)–O(2)	2.155(3)
Mn(1)–O(5)	2.327(4)	Mn(2)–O(3)	2.327(3)
Mn(1)–N(1)	2.098(3)	Mn(2)–O(4)	2.107(3)
Mn(1)–N(2)	2.367(4)	Mn(1)···Mn(2)	3.210(1)
O(1)–Mn(1)–O(2)	169.8(1)	Cl(1)–Mn(2)–O(2)	130.7(1)
O(1)–Mn(1)–O(4)	96.4(1)	Cl(1)–Mn(2)–O(3)	93.1(1)
O(1)–Mn(1)–O(5)	87.2(1)	Cl(1)–Mn(2)–O(4)	106.0(1)
O(1)–Mn(1)–N(1)	94.6(1)	Cl(2)–Mn(2)–O(2)	114.2(1)
O(1)–Mn(1)–N(2)	97.1(1)	Cl(2)–Mn(2)–O(3)	98.1(1)
O(2)–Mn(1)–O(4)	79.3(1)	Cl(2)–Mn(2)–O(4)	106.6(1)
O(2)–Mn(1)–O(5)	83.9(1)	O(2)–Mn(2)–O(3)	69.7(1)
O(2)–Mn(1)–N(1)	90.4(1)	O(2)–Mn(2)–O(4)	70.1(1)
O(2)–Mn(1)–N(2)	92.5(1)	O(3)–Mn(2)–O(4)	138.7(1)
O(4)–Mn(1)–O(5)	93.7(1)	Mn(1)–O(2)–Mn(2)	103.3(1)
O(4)–Mn(1)–N(1)	168.5(1)	Mn(1)–O(2)–C(12)	131.1(3)
O(4)–Mn(1)–N(2)	94.4(1)	Mn(2)–O(2)–C(12)	122.2(3)
O(5)–Mn(1)–N(1)	90.2(1)	Mn(1)–O(4)–Mn(2)	106.2(1)
O(5)–Mn(1)–N(2)	170.3(1)	Mn(1)–O(4)–C(28)	130.4(4)
N(1)–Mn(1)–N(2)	80.8(1)	Mn(2)–O(4)–C(28)	122.7(4)
Cl(1)–Mn(2)–Cl(2)	113.80(7)		

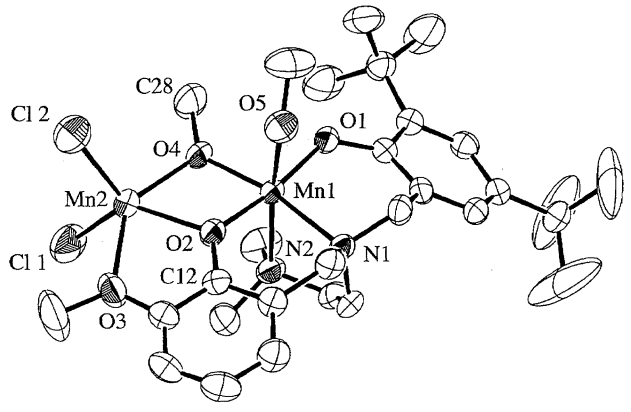

Fig. 4. ORTEP view of $[Mn(L^5)(CH_3OH)(OCH_3)MnCl_2]$ (**4**) with thermal ellipsoids of 50% probability.

As expected from the structure of $[Mn(L^5)(CH_3OH)(OCH_3)MnCl_2]$ (**4**), the electronic absorption spectrum of this complex is similar to that of the trinuclear complex, $[Mn_3(L^2)_2(mcba)_2(OCH_3)_2]$, in dichloromethane (Fig. 5). The intensities are different, since the extinction coefficient is defined as the value per molecule. Both di- and trinuclear complexes show shoulders at about 23×10^3 cm^{-1}, which are assigned to LMCT bands. In a methanol solution, the spectral pattern of **4** changes and an intense new band appears at 20.04×10^3 cm^{-1} (499 nm, $\varepsilon = 2190$ M^{-1} cm^{-1}). A similar band is shown in a dichloromethane solution of the mononuclear complex, $[Mn(L^3)(mcba)(CH_3OH)]$. Besides, the maximum of the LMCT band is at the same position as that for the $[Mn(L^2)(solvent)_2]^+$ cation described above. Therefore this absorption band is attributed to that of the $[Mn(L^5)(solvent)_2]^+$ species generated by dissociation of **4**.

The selectivity of the number of manganese cores in a methanol solution is summarized in Scheme 1. In this system, the 3-positioned *t*-butyl groups remarkably prevent the formation of polynuclear complexes. So the L^3 ligand gives

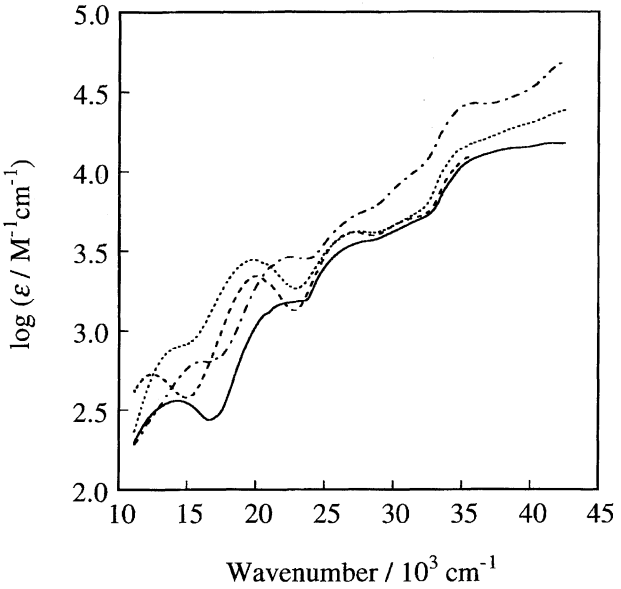

Fig. 5. Electronic absorption spectra of $[Mn(L^5)(CH_3OH)(OCH_3)MnCl_2]$ (**4**) in dichloromethane (—) and in methanol (- - -), $[Mn_3(L^2)_2(mcba)_2(OCH_3)_2]$ (–·–) in dichloromethane, and $[Mn(L^3)(mcba)(CH_3OH)]$ in dichloromethane (····).

only the mononuclear complex. The phenolate oxygen of the other ligands have a bridging ability. Thus, the polynuclear complexes form in methanol under basic conditions, with the phenolato and alkoxo bridges. In the process, the steric interactions of the μ-alkoxo ligand with the R^1 and R^3 substituents are important. The combination of R^1 and R^3 in the tripodal ligand controls the magnitude of the steric interaction (Fig. 3). One point to note is the isolation of the mixed-valence dinuclear complex, $[Mn(L^5)(CH_3OH)(OCH_3)MnCl_2]$ (**4**). The L^5 ligand (R^1 = *t*-Bu and $R^3 = OCH_3$) has a combination of the bulkiest substituents next to the L^3 ligand. Therefore, the L^5 ligand makes it possible to isolate the dinuclear complex, **4**.

Trinuclear Manganese Complexes with Phenolato and Carboxylato Bridges. In the above experiment, the synthesis of polynuclear complexes was carried out in methanol. As a result, all bridging frames of the polynuclear complexes contain alkoxo bridges. This implies that the change in the reaction solvent should make the formation of a different bridging framework possible. Actually, the preparation of polynuclear complexes in acetonitrile afforded diverse bridging frames.

The reaction of the L^1 ligand (1 equiv) with $Mn(ClO_4)_2 \cdot 6H_2O$ (1.5 equiv), benzoic acid (2 equiv), and *N*,*N*-diisopropylethylamine (4 equiv) in acetonitrile gave a trinuclear complex, $[Mn_3(L^1)_2(ba)_4]$ (**5**). The molecular structure is shown in Fig. 6, and the selected bond distances and angles are given in Table 4. This trinuclear complex consists of a central manganese ion and two flanking manganese ions. The central and terminal manganese ions are bridged by two carboxylate ligands and a phenolate group. Therefore, the octahedral coordination environment of the terminal manganese is composed of an N_2O_2 donor set of the tripodal ligand and two oxygen donors of the bridging carboxylate ligands. The carboxylate oxygen donors, O(5) and O(9), occupy the equatorial plane. The bond distances of 1.975(9) (Mn(1)–O(5)) and 1.994(8) Å (Mn(3)–O(9)) are comparable to that of Mn–O(carboxylato) in the mononuclear complex, $[Mn(L^3)(mcba)(CH_3OH)]$. The other Mn–O(carboxylato) distances in axial directions are 2.098(8) (Mn(1)–O(7)) and 2.109(9) Å (Mn(3)–O(11)), and larger than those in the equatorial plane. The structure around the flanking manganese ions are similar

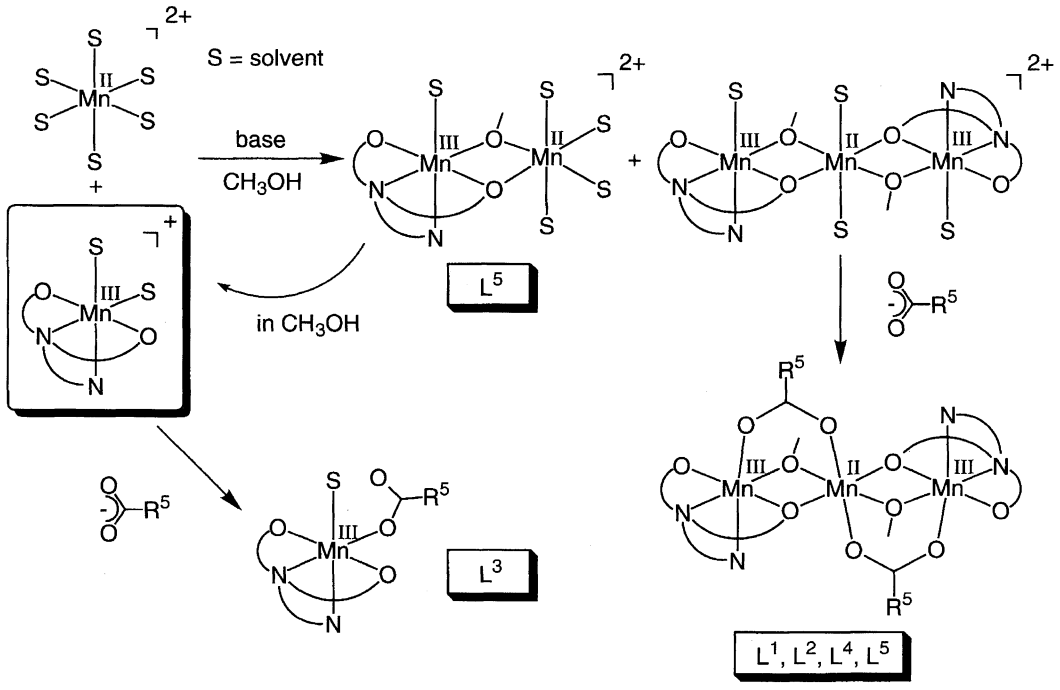

Scheme 1.

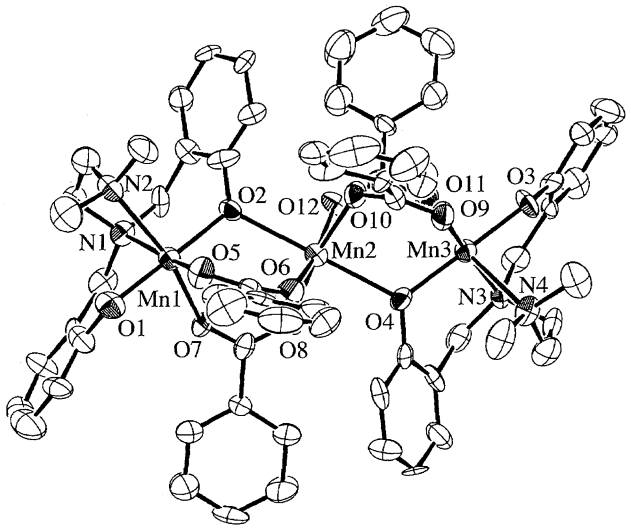

Fig. 6. ORTEP view of $[Mn_3(L^1)_2(ba)_4]$ (**5**) with thermal ellipsoids of 50% probability.

to those of the manganese(III) site surrounded by the tripodal tetradentate ligand (L) in other related complexes. The octahedral coordination environment of the central manganese is composed of four oxygen donors of the μ-carboxylato ligands and two oxygen donors at the phenolato bridges from the tripodal ligands. The large Mn–O(phenolato) distances, 2.319(8) (Mn(2)–O(2)) and 2.296(8) Å (Mn(2)–O(4)), reflect that this trinuclear complex is crowded with the four carboxylato bridges. As in the case of $[Mn_3(L)_2(carboxylato)_2(OCH_3)_2]$, the oxidation state of the central core (Mn(2)) is assigned to Mn^{II}, and those of the flanking cores (Mn(1) and Mn(3)) are assigned to Mn^{III}.[8] These three manganese cores are almost linearly arranged (the Mn(1)···Mn(2)···Mn(3) angle is 168.67(8)°).

Trinuclear Manganese Complexes with Phenolato, Carboxylato, and Hydroxo Bridges. The reaction of the L^2 ligand (1 equiv) with $Mn(ClO_4)_2 \cdot 6H_2O$ (1.5 equiv), benzoic acid (2 equiv), and *N,N*-diisopropylethylamine (4 equiv) in acetonitrile gave a dark brown product. The IR spectrum of this compound is very similar to that of $[Mn_3(L^2)_2(ba)_2(OCH_3)_2]$, except that a sharp signal was observed at 3662 cm^{-1}. This implies that this compound includes a hydroxo ligand with no hydrogen bond. When the compound was treated with D_2O, a new signal appeared at 2702 cm^{-1}, which is assigned to the O–D com-

Table 4. Selected Bond Distances (Å) and Angles (deg) for $[Mn_3(L^1)_2(ba)_4]$ (**5**)

Mn(1)–O(1)	1.854(9)	Mn(2)–O(12)	2.128(9)
Mn(1)–O(2)	1.933(8)	Mn(3)–O(3)	1.864(8)
Mn(1)–O(5)	1.975(9)	Mn(3)–O(4)	1.941(8)
Mn(1)–O(7)	2.098(8)	Mn(3)–O(9)	1.994(8)
Mn(1)–N(1)	2.14(1)	Mn(3)–O(11)	2.109(9)
Mn(1)–N(2)	2.43(1)	Mn(3)–N(3)	2.11(1)
Mn(2)–O(2)	2.319(8)	Mn(3)–N(4)	2.42(1)
Mn(2)–O(4)	2.296(8)	Mn(1)···Mn(2)	3.556(3)
Mn(2)–O(6)	2.169(9)	Mn(2)···Mn(3)	3.574(3)
Mn(2)–O(8)	2.107(9)	Mn(1)···Mn(3)	7.095(3)
Mn(2)–O(10)	2.123(9)		
O(1)–Mn(1)–O(2)	179.7(4)	O(4)–Mn(2)–O(12)	99.0(3)
O(1)–Mn(1)–O(5)	88.3(4)	O(6)–Mn(2)–O(8)	94.1(4)
O(1)–Mn(1)–O(7)	87.7(4)	O(6)–Mn(2)–O(10)	85.5(4)
O(1)–Mn(1)–N(1)	88.2(4)	O(6)–Mn(2)–O(12)	169.3(4)
O(1)–Mn(1)–N(2)	83.2(4)	O(8)–Mn(2)–O(10)	170.1(4)
O(2)–Mn(1)–O(5)	91.8(4)	O(8)–Mn(2)–O(12)	93.6(3)
O(2)–Mn(1)–O(7)	92.6(4)	O(10)–Mn(2)–O(12)	88.2(3)
O(2)–Mn(1)–N(1)	91.5(4)	O(3)–Mn(3)–O(4)	178.9(4)
O(2)–Mn(1)–N(2)	96.5(4)	O(3)–Mn(3)–O(9)	90.4(4)
O(5)–Mn(1)–O(7)	102.4(4)	O(3)–Mn(3)–O(11)	86.3(4)
O(5)–Mn(1)–N(1)	167.9(4)	O(3)–Mn(3)–N(3)	87.9(4)
O(5)–Mn(1)–N(2)	87.7(4)	O(3)–Mn(3)–N(4)	85.3(4)
O(7)–Mn(1)–N(1)	89.1(4)	O(4)–Mn(3)–O(9)	89.8(4)
O(7)–Mn(1)–N(2)	166.1(4)	O(4)–Mn(3)–O(11)	92.5(4)
N(1)–Mn(1)–N(2)	80.3(4)	O(4)–Mn(3)–N(3)	92.2(4)
O(2)–Mn(2)–O(4)	172.0(3)	O(4)–Mn(3)–N(4)	95.8(4)
O(2)–Mn(2)–O(6)	84.4(3)	O(9)–Mn(3)–O(11)	100.6(4)
O(2)–Mn(2)–O(8)	97.8(3)	O(9)–Mn(3)–N(3)	169.6(4)
O(2)–Mn(2)–O(10)	91.9(3)	O(9)–Mn(3)–N(4)	88.5(4)
O(2)–Mn(2)–O(12)	87.2(3)	O(11)–Mn(3)–N(3)	89.5(4)
O(4)–Mn(2)–O(6)	88.8(3)	O(11)–Mn(3)–N(4)	167.7(4)
O(4)–Mn(2)–O(8)	86.8(3)	N(3)–Mn(3)–N(4)	81.1(4)
O(4)–Mn(2)–O(10)	83.3(3)	Mn(1)···Mn(2)···Mn(3)	168.67(8)

pression. Consequently, the compound was assigned to a trinuclear complex, $[Mn_3(L^2)_2(ba)_2(OH)_2]$ (**6**), in which the hydroxo bridges are introduced at the μ-alkoxo positions of $[Mn_3(L^2)_2(ba)_2(OCH_3)_2]$. Since the L^2 ligand has the 3-positioned *t*-butyl group, the structure analogous to $[Mn_3(L^1)_2(ba)_4]$ (**5**) should be sterically crowded. Thus the two bridging carboxylato ligands are replaced by two hydroxo bridges. On the other hand, the reaction in acetonitrile on the L^3 ligand gave a mononuclear complex, $[Mn(L^3)(mcba)(H_2O)]$ (**7**), as with $[Mn(L^3)(mcba)(CH_3OH)]$ produced in methanol. These results also indicate that the 3-positioned *t*-butyl group on the tripodal ligands prevents the bridging of the phenolate oxygen donor.

Tetranuclear Manganese Complex with Phenolato and Carboxylato Bridges. The L^5 ligand gave a tetranuclear manganese complex in acetonitrile. The tetranuclear complex, $[Mn_4(L^5)_2(ba)_6]$ (**8**), is regarded as a dimer of a mixed-valence dinuclear complex. Figure 7 shows the molecular structure of **8**. Two central carboxylate ligands bridge the two dinuclear units which are connected by a crystallographic inversion center, and the other carboxylate ligands are used for constructing the independent dimanganese units. The structure of the dimanganese unit resembles the $Mn^{III}\cdots Mn^{II}$ moiety of the trinuclear complex **5**. Thus, the two terminal Mn cores surrounded by the L^5 ligands are in the trivalent oxidation state, and the two central Mn cores are in the divalent one. Consequently, the tetranuclear system in complex **8** consists of an almost linear $Mn^{III}\cdots Mn^{II}\cdots Mn^{II}\cdots Mn^{III}$ arrangement. Selected bond distances and angles are given in Table 5. The distance between the manganese(III) and manganese(II) ions is 3.596(3) Å, and is comparable to that of **5** (3.57 Å). The two manganese(II) ions are largely separated (4.835(4) Å).

Scheme 2 summarizes how the manganese complexes are selectively formed in acetonitrile. As described in the dinuclear complex **4**, the L^5 ligand with the *t*-butyl group (R^1) and the methoxy group (R^3) prevents the formation of trinuclear complexes such as $[Mn_3(L^1)_2(ba)_4]$ and $[Mn_3(L^2)_2(ba)_2(OH)_2]$. As a result, the favorable dinuclear units, $[Mn(L^5)(ba)_2Mn]^+$, are connected with the two carboxylate ligands to produce the tetranuclear complex.

Table 5. Selected Bond Distances (Å) and Angles (deg) for $[Mn_4(L^5)_2(ba)_6]$ (**8**)

Mn(1)–O(1)	1.871(8)	Mn(2)–O(3)	2.509(9)
Mn(1)–O(2)	1.916(8)	Mn(2)–O(5)	2.124(9)
Mn(1)–O(4)	1.987(9)	Mn(2)–O(7)	2.123(9)
Mn(1)–O(6)	2.120(9)	Mn(2)–O(8)	2.125(9)
Mn(1)–N(1)	2.12(1)	Mn(2)–O(9*)	2.073(8)
Mn(1)–N(2)	2.41(1)	Mn(1)···Mn(2)	3.596(3)
Mn(2)–O(2)	2.216(8)	Mn(2)···Mn(2*)	4.835(4)
O(1)–Mn(1)–O(2)	175.2(4)	O(2)–Mn(2)–O(3)	67.3(3)
O(1)–Mn(1)–O(4)	85.4(4)	O(2)–Mn(2)–O(5)	84.9(3)
O(1)–Mn(1)–O(6)	87.6(4)	O(2)–Mn(2)–O(7)	96.0(3)
O(1)–Mn(1)–N(1)	90.6(4)	O(2)–Mn(2)–O(8)	86.8(3)
O(1)–Mn(1)–N(2)	92.9(4)	O(2)–Mn(2)–O(9*)	151.0(3)
O(2)–Mn(1)–O(4)	93.1(3)	O(3)–Mn(2)–O(5)	94.2(4)
O(2)–Mn(1)–O(6)	88.1(3)	O(3)–Mn(2)–O(8)	83.0(3)
O(2)–Mn(1)–N(1)	92.0(3)	O(3)–Mn(2)–O(7)	161.8(3)
O(2)–Mn(1)–N(2)	91.5(4)	O(3)–Mn(2)–O(9*)	85.4(3)
O(4)–Mn(1)–O(6)	95.9(4)	O(5)–Mn(2)–O(7)	91.4(4)
O(4)–Mn(1)–N(1)	164.7(4)	O(5)–Mn(2)–O(8)	171.7(4)
O(4)–Mn(1)–N(2)	86.9(4)	O(5)–Mn(2)–O(9*)	87.8(3)
O(6)–Mn(1)–N(1)	98.7(4)	O(7)–Mn(2)–O(8)	89.0(4)
O(6)–Mn(1)–N(2)	177.3(4)	O(7)–Mn(2)–O(9*)	112.2(4)
N(1)–Mn(1)–N(2)	78.6(4)	O(8)–Mn(2)–O(9*)	99.7(3)

Magnetic Properties. As reported in the preceding paper, the Mn^{III}–Mn^{II}–Mn^{III} systems of general formula $[Mn_3(L)_2(carboxylato)_2(OCH_3)_2]$, which consists of the carboxylato, phenolato, and alkoxo bridges, have weak spin exchange interactions.[8] In those cases, both antiferromagnetic and ferromagnetic spinexchange couplings appeared. The exchange interaction of this system may exist around the border between antiferromagnetic and ferromagnetic interactions. The sign is influenced by a small change of the structural or electronic environment. This was clearly shown by the comparison between $[Mn_3(L^1)_2(mcba)_2(OC_2H_5)_2]$ (**9**) and $[Mn_3(L^6)_2(mcba)_2(OC_2H_5)_2]$ (**10**). These two complexes are different only in the axial ligands of the ter-

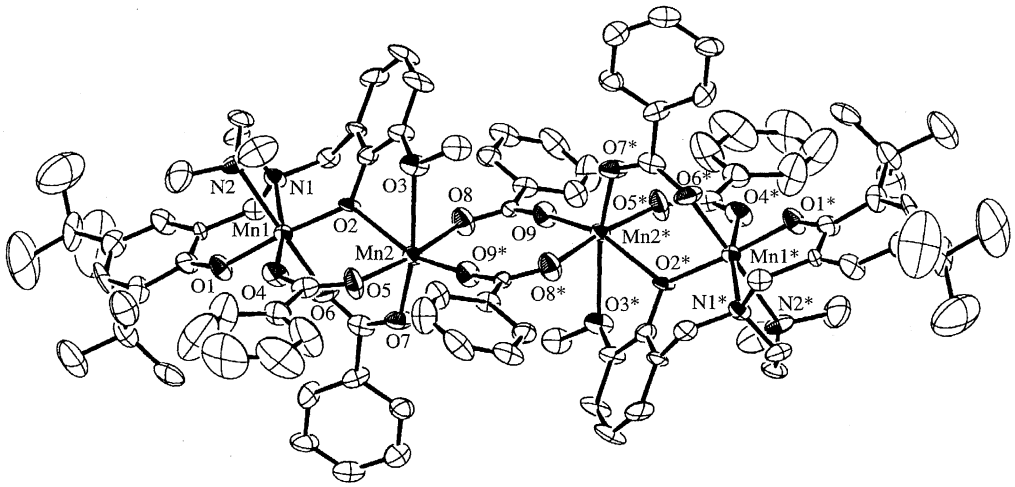

Fig. 7. ORTEP view of $[Mn_4(L^5)_2(ba)_6]$ (**8**) with thermal ellipsoids of 50% probability.

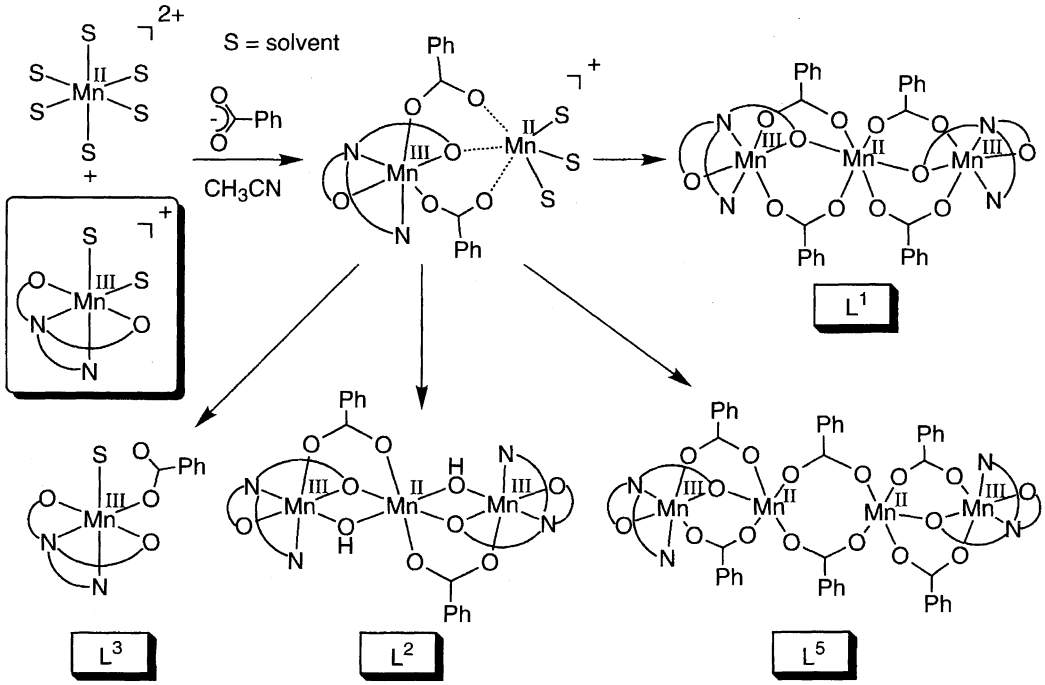

Scheme 2.

minal manganese(III) ions (the tertiary amine nitrogen of **9** and the pyridine nitrogen of **10**). However, the temperature-dependent magnetic behavior indicates the ferromagnetic spin-exchange interaction for **9** and the antiferromagnetic spin-exchange interaction for **10** (Fig. 8). The spin Hamiltonian in trinuclear complexes is expressed as $H = -2[J_{12}(S_1 \cdot S_2) + J_{23}(S_2 \cdot S_3) + J_{31}(S_3 \cdot S_1)]$ where $S_1 = S_3 = 2$ and $S_2 = 5/2$ for the S_1–S_2–S_3 arrangement. As reported in the preceding paper, in these trinuclear complexes, the equivalent environment was assumed for the terminal manganese(III) ions.[8] Therefore, the spin-exchange interaction between Mn^{III} and Mn^{II} is designated as $J = J_{12} = J_{23}$. Because a large $Mn^{III} \cdots Mn^{III}$ distance is expected, the interaction between the terminal manganese(III) ions can be excluded ($J_{13} = 0$). A theoretical expression for the molar magnetic susceptibility is derived using the Kambe vector-coupling method[16] and the Van Vleck equation. In compound **9**, a slight decrease in the effective magnetic moment at 2—3.5 K is presumed to be contribution from an intermolecular interaction and/or zero-field splitting terms. The effect was included in parameter θ (replacing T in the theoretical expression with $T-\theta$). The curve fittings were employed for three parameters of J, g (the average g value), and θ. The minimized function was $\sum[(\mu_{eff})_{exptl} - (\mu_{eff})_{calcd}]^2$. The best fitting parameters were $J = 0.65$ cm^{-1}, $g = 1.99$, and $\theta = -0.56$ K for **9**. For complex **10**, no good fitting was obtained. Thus the fitting was carried out using a fixed g value of 2.0. As a result, the J value was -0.23 cm^{-1}.

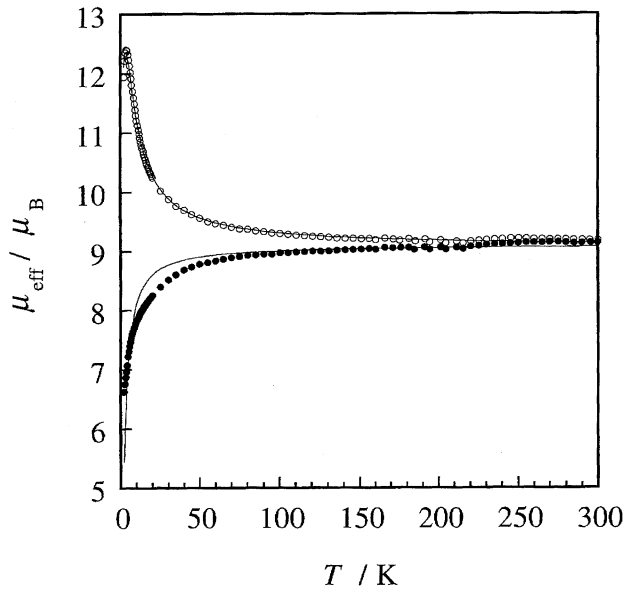

Fig. 8. Temperature dependence of the magnetic moments per molecule of $[Mn_3(L^1)_2(mcba)_2(OC_2H_5)_2]$ (**9**) (○) and $[Mn_3(L^6)_2(mcba)_2(OC_2H_5)_2]$ (**10**) (●). Solid lines represent the least-squares fits.

Clearly, both antiferromagnetic and ferromagnetic superexchange pathways contribute to the overall magnetic interaction between the Mn^{III} and Mn^{II} cores. However, the presence of three different bridging ligands complicate the pathways. If the major character of the magnetic interaction is dominated by the combination of the bridging ligands, $[Mn(L^5)(CH_3OH)(OCH_3)MnCl_2]$ (**4**) and $[Mn_3(L^1)_2(ba)_4]$ (**5**) will serve to understand the superexchange pathways. The former has the phenolato and alkoxo bridges, and the latter has the phenolato and two carboxylato bridges.

Temperature-dependent molar susceptibility measurements of powdered samples of the dinuclear complex, $[Mn(L^5)(CH_3OH)(OCH_3)MnCl_2]$ (**4**), were carried out in the temperature range 2—300 K (Fig. 9). The effective mag-

netic moment increases from 8.06 μ_B at 295 K to 10.26 μ_B at 5.0 K. This indicates a ferromagnetic coupling between the electronic spins of Mn^{III} and Mn^{II} ions. The magnetic data were analyzed using the isotropic spin-exchange coupling model. The spin Hamiltonian in dinuclear complexes is expressed as $H = -2J(S_1 \cdot S_2)$ where $S_1 = 2$ and $S_2 = 5/2$. The spin-exchange coupling constant for the Mn^{III}–Mn^{II} interactions is expressed as J. A theoretical expression for the molar magnetic susceptibility is derived using the Kambe vector-coupling method[16] and the Van Vleck equation. The curve fittings were employed for two parameters of J and g (the average g value). A slight decrease in the effective magnetic moment at 2—5 K cannot be interpreted by the introduction of the parameter θ. The best fits were obtained with $J = 3.02$ cm^{-1} and $g = 2.04$. Similar weak ferromagnetic coupling between Mn^{III} and Mn^{II} has been reported for dinuclear complexes with two phenolato bridges ($J = 0.86$ cm^{-1})[17] and with two alkoxo bridges ($J = 3.23$ cm^{-1}).[18] In the former, a slight decrease in the effective magnetic moment at low temperature was interpreted using the zero-field splitting parameters of the Mn^{II} and Mn^{III} ions. The spin-exchange coupling constant of **4** is larger than those for the trinuclear complexes with the Mn^{III}–Mn^{II}–Mn^{III} arrangement, $[Mn_3(L)_2(carboxylato)_2(OCH_3)_2]$, of which the spin-exchange coupling constants range from -0.25 to 1.9 cm^{-1}.[8] As described above, the dinuclear structure consisting of the phenolato and alkoxo bridges in **4** is similar to those consisting of the phenolato, alkoxo, and carboxylato bridges in the trinuclear complexes $[Mn_3(L)_2(carboxylato)_2(OCH_3)_2]$. Consequently, the contributions of the phenolato and alkoxo bridges to the magnetic coupling are ferromagnetic.

In the mixed-valence trinuclear complex, $[Mn_3(L^1)_2(ba)_4]$ (**5**), the Mn^{II} and Mn^{III} cores interact antiferromagnetically. The temperature-dependence of magnetic susceptibility was measured, and the effective magnetic moment is shown in Fig. 10. The experimental data were fitted with the two parameters, J and g, which are based on the same theoretical treatment for compound **9**. The exchange coupling constant between Mn^{III} and Mn^{II} is -3.35 cm^{-1}, and $g = 2.02$. Similar mixed-valence trinuclear manganese complexes have been reported, and exhibit antiferromagnetic spin-exchange interactions (-7.1——-4.0 cm^{-1}).[5—7] In those complexes, the Mn^{III} and Mn^{II} are bridged by two carboxylate and one alkoxide groups. Therefore, most of the Mn^{III}–Mn^{II}–Mn^{III} complexes containing carboxylato bridges show antiferromagnetic interactions between Mn^{III} and Mn^{II}. This trend is also seen for the Mn^{III}–Mn^{II} dinuclear complexes.[19—22] These antiferromagnetic interactions through the carboxylato bridges also exist in **9**, **10**, and the previously reported analogues of the type $[Mn_3(L)_2(carboxylato)_2(OCH_3)_2]$. Accordingly, their ambiguous weak interactions are interpreted as meaning that the antiferromagnetic contribution of the carboxylato bridge cancel out the ferromagnetic interactions through the phenolato and alkoxo bridges.

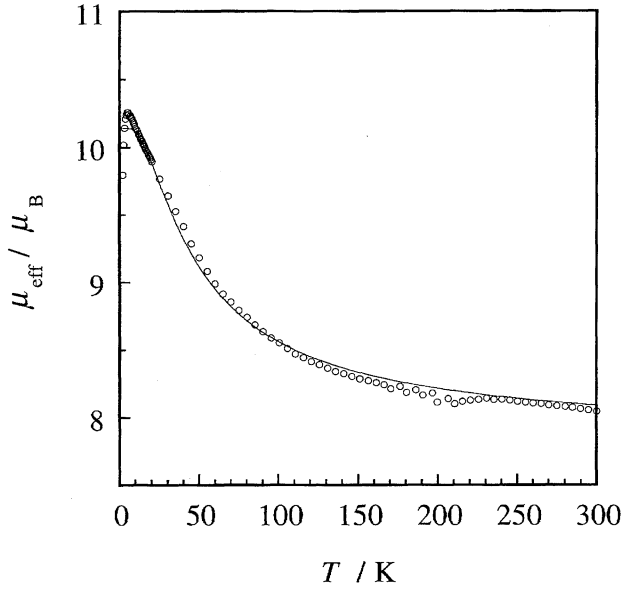

Fig. 9. Temperature dependence of the magnetic moments per molecule of $[Mn(L^5)(CH_3OH)(OCH_3)MnCl_2]$ (**4**) (○). A solid line represents the least-squares fit.

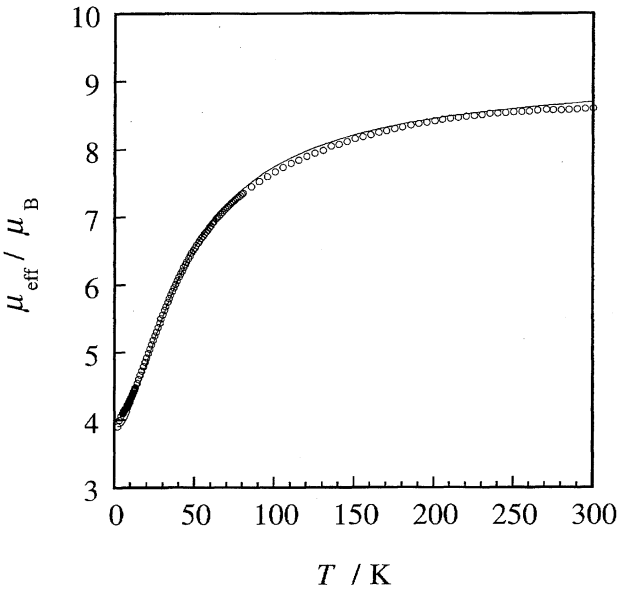

Fig. 10. Temperature dependence of the magnetic moments per molecule of $[Mn_3(L^1)_2(ba)_4]$ (**5**) (○). A solid line represents the least-squares fit.

The authors wish to thank Dr. Satoshi Takamizawa for technical assistance in the magnetic studies. The authors also thank Institute for Molecular Science for the use of a diffractometer.

References

1) V. L. Pecoraro, M. J. Baldwin, and A. Gelasco, *Chem. Rev.*, **94**, 807 (1994).

2) V. L. Pecoraro, "Manganese Redox Enzymes," VCH, New York (1992).

3) G. C. Dismukes, *Chem. Rev.*, **96**, 2909 (1996).

4) V. K. Yachandra, K. Sauer, and M. P. Klein, *Chem. Rev.*, **96**, 2927 (1996).

5) V. Tangoulis, D. A. Malamatari, K. Soulti, V. Stergiou, C. P. Raptopoulou, A. Terzis, T. A. Kabanos, and D. P. Kessissoglou, *Inorg. Chem.*, **35**, 4974 (1996).

6) D. A. Maramatari, P. Hitou, A. G. Hatzidimitriou, F. E. Inscore, A. Gourdon, M. L. Kirk, and D. P. Kessissoglou, *Inorg. Chem.*, **34**, 2493 (1995).

7) D. P. Kessissoglou, M. L. Kirk, M. S. Lah, X. Li, C. Raptopoulou, W. E. Hatfield, and V. L. Pecoraro, *Inorg. Chem.*, **31**, 5424 (1992).

8) M. Hirotsu, M. Kojima, and Y. Yoshikawa, *Bull. Chem. Soc. Jpn.*, **70**, 649 (1997).

9) C. J. Hinshaw, G. Peng, R. Singh, J. T. Spence, J. H. Enemark, M. Bruck, J. Kristofzski, S. L. Merbs, R. B. Ortega, and P. A. Wexler, *Inorg. Chem.*, **28**, 4483 (1989).

10) "TEXSAN: Single Crystal Structure Analysis Software," Molecular Structure Corp., The Woodlands, TX, 77381 (1985).

11) A. Neves, S. M. D. Erthal, I. Vencato, A. S. Ceccato, Y. P. Mascarenhas, O. R. Nascimento, M. Hörner, and A. A. Batista, *Inorg. Chem.*, **31**, 4749 (1992).

12) A. Neves, I. Vencato, and S. M. D. Erthal, *Inorg. Chim. Acta*, **262**, 77 (1997).

13) B. Adam, E. Bill, E. Bothe, B. Goerdt, G. Haselhorst, K. Hildenbrand, A. Sokolowski, S. Steenken, T. Weyhermüller, and K. Wieghardt, *Chem. Eur. J.*, **3**, 308 (1997).

14) Y. Zang and L. Que, Jr., *Inorg. Chem.*, **34**, 1030 (1995).

15) Y.-M. Chiou and L. Que, Jr., *J. Am. Chem. Soc.*, **117**, 3999 (1995).

16) K. Kambe, *J. Phys. Soc. Jpn.*, **5**, 48 (1950).

17) A. N. Schake, E. A. Schmitt, A. J. Conti, W. E. Streib, J. C. Huffman, D. N. Hendrickson, and G. Christou, *Inorg. Chem.*, **30**, 3192 (1991).

18) A. Gelasco, M. L. Kirk, J. W. Kampf, and V. L. Pecoraro, *Inorg. Chem.*, **36**, 1829 (1997).

19) R. M. Buchanan, K. J. Oberhausen, and J. F. Richardson, *Inorg. Chem.*, **27**, 971 (1988).

20) H.-R. Chang, H. Diril, M. J. Nilges, X. Zhang, J. A. Potenza, H.-J. Schugar, D. N. Hendrickson, and S. S. Isied, *J. Am. Chem. Soc.*, **110**, 625 (1988).

21) H. Diril, H.-R. Chang, X. Zhang, S. K. Larsen, J. A. Potenza, C. G. Pierpont, H. J. Schugar, S. S. Isied, and D. N. Hendrickson, *J. Am. Chem. Soc.*, **109**, 6207 (1987).

22) M. Suzuki, M. Mikuriya, S. Murata, A. Uehara, H. Oshio, S. Kida, and K. Saito, *Bull. Chem. Soc. Jpn.*, **60**, 4305 (1987).